Environ. Sci. Technol. **2010,** *44,* 6674–6679

Photoreactivity of Carboxylated Single-Walled Carbon Nanotubes in Sunlight: Reactive Oxygen Species Production in Water

CHIA-YING CHEN AND CHAD T. JAFVERT*

Purdue University, School of Civil Engineering, West Lafayette, Indiana 47907

Received April 5, 2010. Revised manuscript received July 9, 2010. Accepted July 21, 2010.

Very limited information exists on transformation processes of carbon nanotubes in the natural aquatic environment. Because the conjugated π-bond structure of these materials is efficient in absorbing sunlight, photochemical transformations are a potential fate process with reactivity predicted to vary with their diameter, chirality, number and type of defects, functionalization, residual metal catalyst and amorphous carbon content, and with the composition of the water, including the type and composition of materials that act to disperse them into the aqueous environment. In this study, the photochemical reactions involving colloidal dispersions of carboxylated single-walled carbon nanotubes (SWNT-COOH) in sunlight were examined. Production of reactive oxygen species (ROS) during irradiation occurs and is evidence for potential further phototransformation and may be significant in assessing their overall environmental impacts. In aerated samples exposed to sunlight or to lamps that emit light only within the solar spectrum, the probe compounds, furfuryl alcohol (FFA), tetrazolium salts (NBT^{2+} and XTT), and *p*-chlorobenzoic acid (*p*CBA), were used to indicate production of $^1O_2$, $O_2^{\cdot-}$, and $\cdot OH$, respectively. All three ROS were produced in the presence of SWNT-COOH and molecular oxygen ($^3O_2$). $^1O_2$ production was confirmed by observing enhanced FFA decay in deuterium oxide, attenuated decay of FFA in the presence of azide ion, and the lack of decay of FFA in deoxygenated solutions. Photogeneration of $O_2^{\cdot-}$ and $\cdot OH$ was confirmed by applying superoxide dismutase (SOD) and tert-butanol assays, respectively. In air-equilibrated suspensions, the loss of 0.2 mM FFA in 10 mg/L SWNT-COOH was ~85% after 74 h. Production of $^1O_2$ was not dependent on pH from 7 to 11; however photoinduced aggregation was observed at pH 3.

Introduction

Since their discovery in 1991, carbon nanotubes (CNTs) have been of great interest to many researchers (*1*). The electronic, thermal, optical, and mechanical properties and the large specific area of carbon nanotubes make them unique for a number of promising applications. However, unfunctionalized carbon nanotubes are extremely hydrophobic and aggregate easily in water. Additionally, it is difficult to prepare them in large quantities with high purity. Dispersions of unfunctionalized (nonderivatized) single-walled carbon nanotubes (u-SWNTs) have been prepared in various organic solvents, including *N,N*-dimethylformamide, *N*-methylpyrrolidone, and 1,2-dichlorobenzene (*2, 3*), and as aqueous dispersions upon addition of various surfactants (e.g., sodium dodecylsulfate (SDS), sodium dodecylbenzene sulfonate (SDBS), and Triton X-100), polymers (*4, 5*), or natural organic matter (*6*). Over the past decade, CNTs have been functionalized (i.e., derivatized) with different hydrophilic moieties that allow them to be dispersed into polar solvents, including water. A common example is simple oxidation under acidic conditions, resulting in the formation of carboxyl groups (−COOH) along their length, that significantly increases their association with water (i.e., decreases the interaction energy). These "water-dispersible" functionalized carbon nanotubes have many potential applications.

Clearly, both unfunctionalized and functionalized CNTs may find widespread use in industry and commerce, and may eventually be released to the environment in ecologically significant amounts. However, compared to the number of studies on potential applications and synthesis of CNTs, the number of studies on their environmental impacts and fate is small (*7*). The various production methods, production levels, types of formulations (i.e., functional group characteristics, chirality, diameter), and applications will impact ecological and human exposure routes and concentrations. These factors also will influence biological responses (i.e., toxicity). For example, cytotoxicity of SWNTs has been reported to be strongly dependent on the sidewall groups (*8*), with the degree and type of agglomeration also an important factor in determining cytotoxicity (*9*). Clearly, further studies on ecotoxicity and environmental impacts are needed for this emerging class of nanomaterials.

The typical length of CNTs suggests that cellular uptake and intracellular transformations are unlikely to play a major role in their environmental fate. Consequently, extracellular redox processes are likely to be important; however the importance of specific redox processes, including the importance of photochemically mediated oxidation in the environment, is currently unknown. Because of structural similarities (i.e., extensive conjugated π-bonds), our recent findings on the photochemical transformations of aqueous C_{60} nanoparticles in sunlight (*10, 11*) suggest that similar reactions may occur for at least some CNT materials. A key intermediate in C_{60} photo-oxidation is singlet oxygen ($^1O_2$) and recent evidence suggests that this excited state may be important in some reactions involving CNTs. For example, SWNT-SiO_2, where SiO_2 particles act as an inert support, suspending in oxygenated D_2O has been shown to generate $^1O_2$ upon laser excitation at 266 nm (*12*). In contrast, it has been reported that (10, 10) SWNTs dissolved in benzene-d_6 were unable to produce or quench $^1O_2$, as evidenced by lack of emission occurring at 1270 nm under irradiation at 200−800 nm (*13*). Photoinduced oxidation of multiwalled CNT (MWNT) films with thicknesses of ~80 μm was reported upon exposure to UV light at λ = 240 nm. The authors indicated that defects on the tube walls may cause the formation of excited triplet states on the CNTs, and suggested that reaction with O_2 produced $^1O_2$ at this wavelength (*14*). SWNTs solubilized in tetrahydrofuran (THF) were found to be photolytically oxidized by $^1O_2$ that was generated using Rose Bengal as the photosensitizer (*15*). This is significant, as other materials in natural waters, including humic acids, generate $^1O_2$. First principle calculations also indicate that $^1O_2$ should react with (8,0) and (6,6) CNTs, and it was further suggested that CNTs with small diameters should degrade

* Corresponding author telephone: (765) 494-2196; fax: (765) 496-1107; e-mail: jafvert@ecn.purdue.edu.

10.1021/es101073p © 2010 American Chemical Society
Published on Web 08/05/2010

upon exposure to air and sunlight (*16*). Recently, $^1O_2$ production was observed upon laser irradiation (at 532 and 355 nm) of carboxylic acid functionalized SWNTs (SWNT-COOH) dispersed in 1:1 D_2O/H_2O and/or modified with chitosan (*17*).

In this study, we report on the production of reactive oxygen species (ROS), including $^1O_2$, via SWNT-COOH under more environmentally relevant conditions. In addition to $^1O_2$, for the first time we provide evidence for production of superoxide anions ($O_2^{\cdot-}$) and hydroxyl radicals (·OH) from SWNT-COOH exposed to sunlight. As we will show, type I and II photosensitization reactions likely occur, with $^1O_2$ produced via energy transfer from SWNT-COOH to O_2, and $O_2^{\cdot-}$ and ·OH photogenerated by electron transfer. ROS production during solar irradiation is critical information for assessing ecological risks of CNTs due to known harmful effects of ROS on cellular materials and because it may provide a pathway through which the photo-oxidation of CNT carbon may occur in the environment.

Experimental Methods

Materials. SWNT-COOH from Carbon Solutions, Inc., containing 1.5−3.0 atomic% carboxylic acid with carbonaceous purity >90%, were used without further purification in most experiments. Methanol was HPLC grade or better, and all chemicals were of the highest purity available and used as received. Furfuryl alcohol (FFA), nitro blue tetrazolium salt (NBT^{2+}), XTT (2,3-Bis(2-methoxy-4-nitro-5-sulfophenyl)-2H-tetrazolium-5-carboxanilide), superoxide dismutase (bovine erythrocytes) (SOD), and *p*-chlorobenzoic acid (*p*CBA) were obtained from Sigma-Aldrich (St. Louis, MO). All water was purified with a Barnstead Nanopure system (Dubuque, IA) after R/O pretreatment.

SWNT-COOH Sample Preparation and Characterization. SWNT-COOH were dispersed in water by sonicating under low energy (8890R-MT, Cole-Parmer, Vernon Hills, IL, operating at 80 W) for 2 h. The suspensions were stable with no phase separation after several weeks of quiescent standing. In some experiments, SWNT-COOH were dispersed in 50 or 100% (v/v) deuterium oxide (D_2O, 99.9%, Cambridge Isotope Laboratories) by the same procedures with all other reagents (e.g., FFA and buffers) prepared in D_2O at the same respective D_2O/H_2O ratio. To investigate the effect of pH on the rate of phototransformation, samples were adjusted to pH = 3, 5, 7, 9, and 11 by adding appropriate phosphate buffers (e.g., H_3PO_4, KH_2PO_4, K_2HPO_4, and Na_3PO_4) to a total phosphate concentration of 5 mM. Accounting for phosphate speciation, sufficient NaCl was added to adjust the ionic strength to 20 mM. For all other experiments, samples were either not buffered (pH ∼ 6) or buffered to pH 7. SWNT-COOH were characterized by transmission electron microscopy (TEM, Philips CM-100 TEM (FEI Company, Hillsboro, OR)). Several images taken from different regions of each sample were evaluated to obtain representative images. Elemental composition of SWNT-COOH materials were measured by scanning electron microscopy (SEM, Nova NanoSEM (FEI Company, Hillsboro, OR)) equipped with an OXFORD INCA 250 electron dispersive X-ray detector (EDX) with parameters of 10 kV, Spot 6, 5.5 mm working distance, and 60 s accumulation time.

Sunlight Irradiation. For most sunlight experiments (West Lafayette, IN, 40°26′ N), samples were placed in borosilicate glass tubes sealed with PTFE-lined caps and exposed to sunlight from 10 a.m. to 4 p.m. on sunny or partly cloudy days. Some samples were wrapped in aluminum foil (dark control samples), and blank control tubes (w/o SWNT-COOH) were prepared in all experiments that examined ROS production. All samples (prepared for each specific sampling time) were prepared in duplicate or triplicate. Samples were uncapped regularly during experiments to ensure $[O_2]$ remained near saturation.

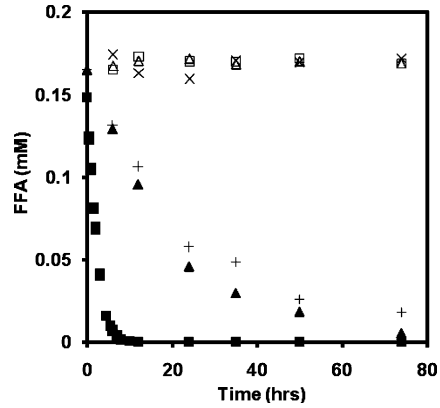

FIGURE 1. FFA loss indicating $^1O_2$ production at pH 7 in lamp light ($\lambda = 350 \pm 50$ nm) by 10 mg/L SWNT-COOH dispersed in D_2O (■), 1:1 D_2O:H_2O (v/v) (▲), and H_2O (+); and FFA recovery in the corresponding dark control samples of D_2O (□), 1:1 D_2O:H_2O (Δ), and H_2O (×).

Lamp Light Irradiation. In some experiments, eight black-light phosphor lamps (RPR-3500 Å, 24 W each, Southern New England Ultraviolet, Branford, CT) were used as an artificial light source. Samples were prepared as described above and irradiated with the lamps in a Rayonet photochemical reactor. The lamps emit only in the solar spectrum over the wavelength range 300 to 410 nm with the maximum photon flux occurring near 350 nm. The light intensity in the reactor was measured with the chemical actinometer potassium ferrioxalate at 2.5×10^{-5} einstein·L^{-1} s^{-1} for 10-mL solution volumes. Sample tubes placed in the Rayonet reactor were rotated by a merry-go-round apparatus at 5 rpm to obtain uniform light exposure.

Reactive Oxygen Species. The production and concentration of different ROS species was monitored using specific scavengers. The production of $^1O_2$ was monitored via the loss of furfuryl alcohol (FFA) (*18*) through which the pseudo-steady-state concentration of $^1O_2$ also was determined (*19*). To detect $O_2^{\cdot-}$, both nitro blue tetrazolium salt (NBT^{2+}) and 2,3-Bis(2-methoxy-4-nitro-5-sulfophenyl)-2H-tetrazolium-5-carboxanilide (XTT) were used, with XTT used with and without superoxide dismutase present in solution (*20, 21*). To detect hydroxyl radicals (·OH), *p*-chlorobenzoic acid (*p*CBA), an ·OH scavenger, was added. Because there are many competitive reactions for ·OH in aqueous solutions (*22*), *p*CBA was added at a very low concentrations (i.e., 2 μM) allowing the pseudo-steady-state concentration of ·OH to be calculated (*23, 24*). A more complete description of the methods used to detect and quantify the ROS is provided in the Supporting Information (SI).

Results and Discussion

Figure 1 shows the loss under lamp light of 0.2 mM FFA in an aqueous suspension of 10 mg/L SWNT-COOH. FFA loss was ∼85% after 74 h of irradiation with no decay occurring in dark control samples. Decay of FFA appears pseudo-first-order and suggests that $^1O_2$ is produced, similar to its production in aqueous clusters of C_{60} (*11*) and fullerol (*25*). The specificity of furfuryl alcohol as a $^1O_2$ probe has been investigated previously (*26*), with the influence of other reactants (e.g., superoxide) claimed to have a negligible effect at FFA concentrations below 10 mM (0.2 mM was used in this study). Because D_2O quenches $^1O_2$ at a slower rate than H_2O (k_d (D_2O) = 1.6×10^4 s^{-1}; k_d (H_2O) = 2.5×10^5 s^{-1}) (*27*), the experiment was performed in D_2O, and in 1:1 D_2O:H_2O for additional confirmation. Consistent with $^1O_2$ production

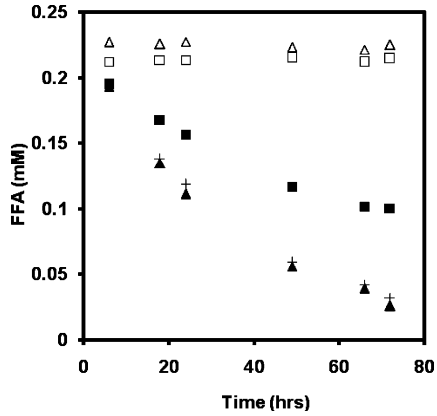

FIGURE 2. FFA loss indicating $^1O_2$ production at pH 7 in lamp light by 10 mg/L SWNT-COOH, containing 10 mM NaN_3 (■), 10 mM NaCl (▲) and without adding ions (+); and FFA recovery in the corresponding dark control samples of NaN_3 (□) and NaCl (Δ).

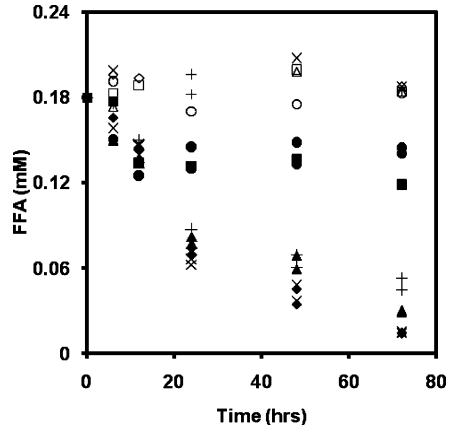

FIGURE 3. $^1O_2$ detection by FFA loss under lamp light in 10 mg/L SWNT-COOH at pH 3 (●), 5 (■), 7 (▲), 9 (×), 11 (♦), and without buffer (+); and FFA recovery in the corresponding dark control samples at pH 3 (○), 5 (□), 7(Δ), 9 (×), 11 (◊), and without buffer (+).

and known quenching trends, FFA loss was 94% in D_2O after 6 h, and 90% and 85% in 50% (v/v) D_2O and H_2O, respectively, after 74 h (Figure 1). Azide ion (N_3^-) quenches singlet oxygen with a second order rate constant of (k_d (N_3^-) = 9×10^8 M^{-1} s^{-1}) (*27*). The rate of FFA loss in samples containing 10 mM azide ion was suppressed by about 40%, further suggesting $^1O_2$ as the ROS species responsible for FFA decay (Figure 2), as decay in the presence of 10 mM NaCl (as as an ionic strength control) showed no effect. Further evidence is the nearly complete quenching of FFA decay upon elimination of O_2, the precursor of $^1O_2$, via degassing with N_2 as shown in Figure S1 (SI). This suggests a type II photosensitization reaction, where photoexcited nanotubes transfer energy directly to O_2. Applying eq S3 (SI), the $^1O_2$ pseudo-steady-state concentration mediated by 10 mg/L SWNT-COOH during a 48 h natural sunlight exposure was calculated at $[^1O_2]_{ss} = 9.95 \times 10^{-14}$ M in water. Correcting the aqueous rate measured in test tubes to that expected for flat open surface waters (a factor of 1.5) and correcting for light attenuation (*19*) results in $[^1O_2]_{ss} = 9.44 \times 10^{-14}$ M expected in a typical natural water due to 10 ppm SWNT-COOH. Under lamp light, $[^1O_2]_{ss} = 8.68 \times 10^{-14}$ in water, 1.11×10^{-13} M in 1:1 D_2O:H_2O, and 1.10×10^{-12} M in D_2O. Using the steady-state value in water under lamp light, the product of $[^1O_2]_{ss} \times (k_d\,(H_2O)/k_d\,(D_2O))$ (= 1.36×10^{-12} M) provides a good estimate for the steady-state $[^1O_2]$ measured in D_2O, as expected.

FFA loss was measured in buffered samples at pH = 3, 5, 7, 9, and 11, and in the absence of buffers (Figure 3). At pH ≥ 7, the FFA decay rate was unaffected by changes in pH; however decay at pH = 3 and 5 was significantly less than that at the higher pH values over the 72 h irradiation period. Importantly, flocculation was observed at pH = 3 and 5 under both lamp light and sunlight, with significant settling of floc occurring in the irradiated pH 3 samples (Figure 4). In lamp light, flocculation occurred after ~6 h at pH 3, and later for samples at pH 5, resulting in inhibition of further FFA decay (i.e., attenuation of $^1O_2$ production). Negligible flocculation occurred in dark control samples at pH 3. At pH 3, a fraction of the acid functional groups on SWNT-COOH will be protonated, reducing charge repulsion between tubes. A potential reason for the observed flocculation in the irradiated samples is photochemical oxidation via oxidative decarboxylation that would further reduce (beyond partial protonation) charge repulsion between the carbon nanotubes allowing them to aggregate. This hypothesis is consistent with zeta potential measurements (Table S1 in SI) of lamp light-irradiated samples and dark control samples that indict a less negative charge on irradiated nanotubes, even though the pH after irradiation is slightly higher. Also, microscopic

FIGURE 4. Photograph of 10 mg/L SWNT-COOH in water at pH 3: A sample irradiated with lamp light (λ = 350 ± 50 nm) for 6 h is on the left and the dark control sample is on the right.

changes (Figure S2 in SI) and visual flocculation (Figure S3 in SI) were evident in samples containing no buffer after exposure to sunlight for 360 h. It is unknown if the metal impurities play a role in the observed photosensitized flocculation at low pH.

To test for possible formation of $O_2^{\cdot-}$, nitro blue tetrazolium salt (NBT^{2+}) was used. The purple monoformazan product of NBT^{2+} reduction by $O_2^{\cdot-}$ was visibly evident in irradiated samples, as also evidenced by the increase in light absorption at 530 nm (Figure 5). Due to the lengthy time period of irradiation, an increase in light absorption also occurred in irradiated NBT^{2+} control tubes (w/o SWNT-COOH) however to a lesser degree than samples containing SWNT-COOH and NBT^{2+}, suggesting production of $O_2^{\cdot-}$ occurred. All dark control samples (Figure 5) had negligible changes in absorbance over the entire UV−vis spectra during irradiation.

XTT was used for further confirmation of $O_2^{\cdot-}$ production. It has the advantage that its reaction with $O_2^{\cdot-}$ can be completely quenched in the presence of superoxide dismutase (SOD) (*20, 21*), and unlike NBT^{2+}, its reduction product is more soluble in water, making quantitative assessment less problematic. In suspensions of SWNT-COOH containing XTT exposed to lamp light, an increase in absorbance occurs where the XTT reduction product has an absorbance maximum (i.e., 470 nm) (Figure 6). Addition of SOD

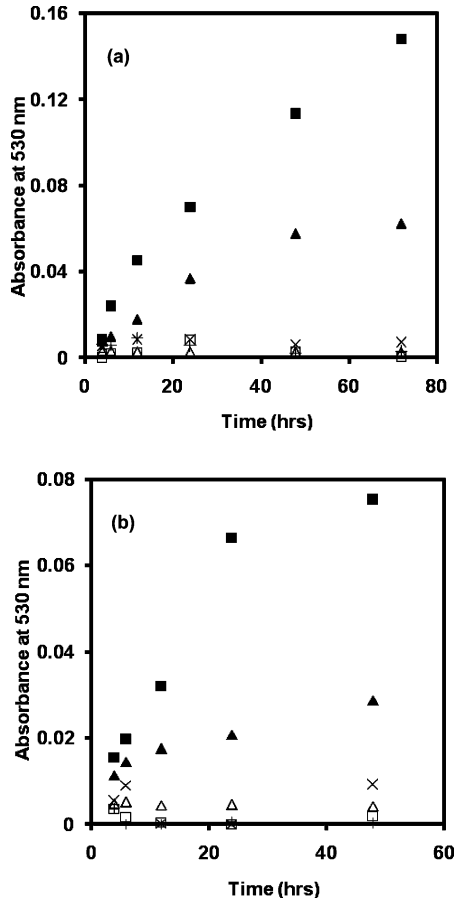

FIGURE 5. Evidence of $O_2^{\cdot-}$ production, via NBT^{2+} (0.2 mM) product formation induced by 10 mg/L SWNT-COOH at pH 7 under (a) lamp light and (b) sunlight. Symbols represent samples containing SWNT-COOH and NBT^{2+} (■), NBT^{2+} alone (▲), and SWNT-COOH alone (+); and the corresponding dark control samples of SWNT-COOH and NBT^{2+} (□), NBT^{2+} alone (Δ), and SWNT-COOH alone (×).

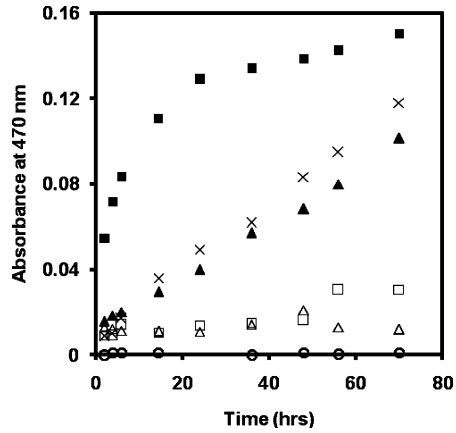

FIGURE 6. Evidence of $O_2^{\cdot-}$ production via XTT (0.1 mM) product formation in suspensions of 10 mg/L SWNT-COOH at pH 7 under lamp light. Symbols represent samples containing SWNT-COOH and XTT (■), SWNT-COOH, XTT, and superoxide dismutase (40 U/mL) (▲), XTT alone (×), and SWNT-COOH alone (○); and the corresponding dark control samples of SWNT-COOH and XTT (□), and SWNT-COOH, XTT, and superoxide dismutase (40 U/mL) (Δ).

completely inhibited XTT reduction, further indicating that $O_2^{\cdot-}$ is the responsible agent for XTT transformation, and that either SWNT-COOH and/or metal impurities (remaining from nanotube production) serve as the electron donor in

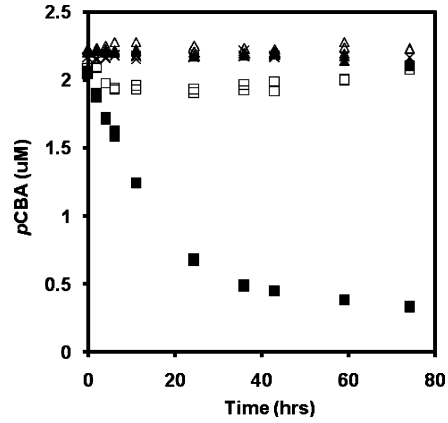

FIGURE 7. Detection of ·OH induced by 10 mg/L SWNT-COOH using *p*CBA as the ·OH scavenger at pH 7 under lamp light, for SWNT-COOH containing *p*CBA (2 μM) (■), *p*CBA alone (2 μM) (▲), and SWNT-COOH containing *p*CBA (2 μM) and tert-butanol (30 mM) (×); and in the corresponding dark control samples of SWNT-COOH containing *p*CBA (2 μM) (□), and *p*CBA alone (2 μM) (Δ).

a type I photochemical reaction. While no studies have previously reported production of other ROS (e.g., $O_2^{\cdot-}$ and ·OH) by SWNT-COOH, the nanotube-mediated generation of $O_2^{\cdot-}$ (and ·OH) can be compared to that generated from unfunctionalized SWNTs (u-SWNTs), reported by Joshi et al. (*28*), in which u-SWNTs, produced by chemical vapor deposition (Thomas Swan & Co.), were irradiated continuously with near-infrared laser (NIR) light centered at 975.5 nm, leading to both $O_2^{\cdot-}$ and ·OH production, as evidenced by deactivation of proteins

$$CNT_{red} \xrightarrow{O_2,\ h\nu} CNT_{ox} + O_2^{\bullet-} \quad (1)$$

No detectable $^1O_2$ was observed in their system, likely due to the low energy of the NIR irradiation (29.17 kcal/mol) compared to the energy required to excite ground state oxygen to the singlet state (22.50 kcal/mol), especially given that the associated electron transitions in the carbon are not 100% efficient.

The free energy change for electron withdrawal by O_2 from semiconducting u-SWNT with diameters of 1.0−1.2 nm is estimated at 7.68−13.37 kcal/mol (*28, 29*). Under our lamp light at the maximum photon flux at 350 nm, the incident photons have an energy of 3.56 eV (i.e., 82.13 kcal/mol) indicating electron withdrawal, even from small diameter u-SWNT is energetically feasible. Functionalization results in "structural defects" on the graphene surface altering electronic properties (*30, 31*). Theoretical calculations indicate that the presence of specific structural defects such as pentagon and heptagon rings within the overall graphene surface reduce the band gap (*31*) creating more energetically favorable conditions for formation of excited states within SWNTs. Thus, at least some "defects" may be associated with active sites where ROS is produced preferentially (*12, 14*).

Employing *p*CBA as a reactive ·OH scavenger, Figure 7 shows *p*CBA decay (2 μM) in 10 mg/L SWNT-COOH suspensions in lamp light. No *p*CBA loss occurred in irradiated samples containing only *p*CBA (i.e., no SWNT-COOH) nor in any dark control samples, suggesting *p*CBA loss occurred by reaction with ·OH. This hypothesis is supported by results obtained by adding to the system 30 mM tert-butanol, a hydroxyl radical quencher that completely inhibited *p*CBA decay due to its rapid quenching at high concentration. Applying eq S4 (SI) to the data, the steady-state concentration of ·OH was calculated at 2.1×10^{-15} M. As mentioned,

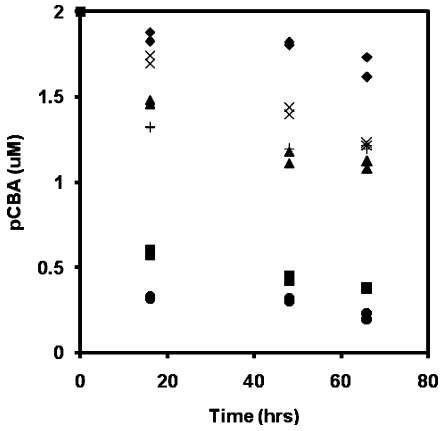

FIGURE 8. *p*CBA loss under lamp light in 10 mg/L SWNT-COOH at pH 3 (●), 5 (■), 7(▲), 9 (×), 11 (♦), and without buffer (+).

production of ·OH by u-SWNTs under NIR irradiation has been reported (*28*). In addition to formation through $O_2^{\cdot-}$

$$O_2^{\bullet-} + 2H^+ + e^- \rightarrow H_2O_2 \quad (2)$$

$$H_2O_2 + H^+ + e^- \rightarrow \cdot OH + H_2O \quad (3)$$

·OH potentially may be generated from water or from hydroxide ions (*28*), and as eqs 2−3 indicate, generation through $O_2^{\cdot-}$ should be pH-dependent. pH-Dependency was examined by monitoring *p*CBA decay in an unbuffered solution and in solutions buffering at pH 3, 5, 7, 9, and 11 (Figure 8). The initial rate of *p*CBA decay increased with decreasing pH, consistent with the hydrogen ion dependency of eqs 2−3. Although photoinduced aggregation again was observed at pH 3, *p*CBA decay was greatest at this pH, presumably due in part to a very fast reaction between ·OH and *p*CBA (i.e., 5.2×10^9 M^{-1} s^{-1} (*24*)).

Although these data indicate significant photochemical production of ROS by SWNT-COOH, it should be noted that scalable inexpensive production of pure either unfunctionalized or functionalized (i.e., metal and other impurities free) carbon nanotubes has yet to be achieved. Generally, impurities include transition metal catalysts and other carbonaceous species. Therefore, we cannot rule out the possibility that metallic catalyst and carbonaceous impurities might be involved in some reactions. For the SWNT-COOH material used in this study, the metal impurities are Ni and Y (<8% w/w, see Table S2 in SI), at a weight ratio of Ni/Y = 6/1. Several studies indicate that under some conditions in the absence of light or CNTs, nickel may play a role in ROS formation, including the generation of H_2O_2 (*32*) and ·OH (*33, 34*).

To examine the potential role of metal and carbonaceous impurities, reaction rates of ROS scavengers were compared between as-received (SWNT-COOH) and treated (t-SWNT-COOH) materials. The t-SWNT-COOH was produced from SWNT-COOH by a process detailed in the SI using heat and acid reflux in an attempt to remove much of the amorphous carbon and metal impurities. It was found that t-SWNT-COOH was less readily dispersed in water by sonication and tended to aggregate upon long-term quiescent standing (compared to SWNT-COOH), suggesting the "purification" process might have led to alteration in functionalities (as noted by a significant decrease in oxygen content upon treatment), therefore comparing rates between the as-received and "treated" materials requires taking all material changes into account. The treatment method we employed reduced the oxygen content from 16.5 to 10.4% (w/w), and reduced the Ni and Y content from 6.4 to 2.6% and 1.1 to 0.0% (w/w), respectively (Table S2, SI). As shown in Figures S4−S6, the t-SWNT-COOH material produced no significant $^1O_2$ over 72 h of irradiation; however it displayed no difference in $O_2^{\cdot-}$ production over the SWNT-COOH material, and had an intermediate affect on ·OH production. Again, factors that may or may not contribute to the absence of $^1O_2$ production in the time frame of our experiment included the following: (1) the decrease in amorphous carbon content, (2) the decrease in metal content, (3) a decrease in −COOH functionalization, and (4) the change in the aggregation state—as the aggregation state may play a significant role in $^1O_2$ production. Whether SWNTs are themselves the photosensitizing species for ROS production or whether impurities play a significant role needs further investigation. Importantly, until a preparation process is capable of producing impurity-free CNTs, it is the CNTs containing residual metal and carbonaceous nanoparticles that may have significant environmental relevance.

Collectively, the results of this study strongly support the hypothesis that under natural sunlight and in water, the reactive oxygen species $^1O_2$, $O_2^{\cdot-}$, and ·OH are generated via SWNT-COOH. Continued research is needed to identify changes to the functional group composition upon irradiation, as any changes to functional group number and type will alter CNT physicochemical properties, effecting transport and potentially toxicity in the aquatic environment.

Acknowledgments

The financial support by the United States Environmental Protection Agency (USEPA) under Award RD 83334001 of the STAR grant program is acknowledged. We thank the reviewers and editor for providing useful comments for improving this paper. We thank Dr. Changhe Xiao for technical assistance, and Ms. Debra Sherman at Purdue's Life Science Microscopy Facility for TEM imaging and SEM/EDX analysis.

Supporting Information Available

Additional information as mentioned in the text. This material is available free of charge via the Internet at http://pubs.acs.org.

Literature Cited

(1) Iijima, S. Helical microtubules of graphitic carbon. *Nature* **1991**, *354*, 56–58.
(2) Ausman, K. D.; Piner, R.; Lourie, O.; Ruoff, R. S.; Korobov, M. Organic solvent dispersions of single-walled carbon nanotubes: Toward solutions of pristine nanotubes. *J. Phys. Chem. B* **2000**, *104*, 8911–8915.
(3) Bahr, J. L.; Mickelson, E. T.; Bronikowski, M. J.; Smalley, R. E.; Tour, J. M. Dissolution of small diameter single-wall carbon nanotubes in organic solvents. *Chem. Commun.* **2001**, 193–194.
(4) Islam, M. F.; Rojas, E.; Bergey, D. M.; Johnson, A. T.; Yodh, A. G. High weight fraction surfactant solubilization of single-wall carbon nanotubes in water. *Nano Lett.* **2003**, *3*, 269–273.
(5) Matarredona, O.; Rhoads, H.; Li, Z. R.; Harwell, J. H.; Balzano, L.; Resasco, D. E. Dispersion of single-walled carbon nanotubes in aqueous solutions of the anionic surfactant naddbs. *J. Phys. Chem. B* **2003**, *107*, 13357–13367.
(6) Hyung, H.; Fortner, J. D.; Hughes, J. B.; Kim, J. H. Natural organic matter stabilizes carbon nanotubes in the aqueous phase. *Environ. Sci. Technol.* **2007**, *41*, 179–184.
(7) Helland, A.; Wick, P.; Koehler, A.; Schmid, K.; Som, C. Reviewing the environmental and human health knowledge base of carbon nanotubes. *Environ. Health Perspect.* **2007**, *115*, 1125–1131.
(8) Sayes, C. M.; Liang, F.; Hudson, J. L.; Mendez, J.; Guo, W. H.; Beach, J. M.; Moore, V. C.; Doyle, C. D.; West, J. L.; Billups, W. E.; Ausman, K. D.; Colvin, V. L. Functionalization density dependence of single-walled carbon nanotubes cytotoxicity in vitro. *Toxicol. Lett.* **2006**, *161*, 135–142.
(9) Wick, P.; Manser, P.; Limbach, L. K.; Dettlaff-Weglikowska, U.; Krumeich, F.; Roth, S.; Stark, W. J.; Bruinink, A. The degree and kind of agglomeration affect carbon nanotube cytotoxicity. *Toxicol. Lett.* **2007**, *168*, 121–131.

(10) Hou, W.-C.; Jafvert, C. T. Photochemical transformation of aqueous C_{60} clusters in sunlight. *Environ. Sci. Technol.* **2009**, *43*, 362–367.
(11) Hou, W.-C.; Jafvert, C. T. Photochemistry of aqueous c_{60} clusters: Evidence of $^1O_2$ formation and its role in mediating C_{60} phototransformation. *Environ. Sci. Technol.* **2009**, *43*, 5257–5262.
(12) Alvaro, M.; Atienzar, P.; Bourdelande, J. L.; Garcia, H. Photochemistry of single wall carbon nanotubes embedded in a mesoporous silica matrix. *Chem. Commun.* **2002**, *24*, 3004–3005.
(13) Baran, P. S.; Khan, A. U.; Schuster, D. I.; Wilson, S. R. Some photophysical properties of nanotubes. *Fullerene Sci. Technol.* **1999**, *7*, 921–925.
(14) Savage, T.; Bhattacharya, S.; Sadanadan, B.; Gaillard, J.; Tritt, T. M.; Sun, Y. P.; Wu, Y.; Nayak, S.; Car, R.; Marzari, N.; Ajayan, P. M.; Rao, A. M. Photoinduced oxidation of carbon nanotubes. *J. Phys.: Condens. Matter* **2003**, *15*, 5915–5921.
(15) Harnon, M. A.; Stensaas, K. L.; Sugar, M. A.; Tumminello, K. C.; Allred, A. K. Reacting soluble single-walled carbon nanotubes with singlet oxygen. *Chem. Phys. Lett.* **2007**, *447*, 1–4.
(16) Chan, S. P.; Chen, G.; Gong, X. G.; Liu, Z. Oxidation of carbon nanotubes by singlet O_2. *Phys. Rev. Lett.* **2003**, *90*, 086403.
(17) Gandra, N.; Chiu, P. L.; Li, W. B.; Anderson, Y. R.; Mitra, S.; He, H. X.; Gao, R. M. Photosensitized singlet oxygen production upon two-photon excitation of single-walled carbon nanotubes and their functionalized analogues. *J. Phys. Chem. C* **2009**, *113*, 5182–5185.
(18) Haag, W. R.; Hoigne, J.; Gassman, E.; Braun, A. M. Singlet oxygen in surface waters. 1. Furfuryl alcohol as a trapping agent. *Chemosphere* **1984**, *13*, 631–640.
(19) Haag, W. R.; Hoigne, J. Singlet oxygen in surface waters. 3. Photochemical formation and steady-state concentrations in various types of waters. *Environ. Sci. Technol.* **1986**, *20*, 341–348.
(20) Ukeda, H.; Maeda, S.; Ishii, T.; Sawamura, M. Spectrophotometric assay for superoxide dismutase based on tetrazolium salt 3′-{1-[(phenylamino)-carbonyl]-3,4-tetrazolium}-bis(4-methoxy-6-nitro)be nzenesulfonic acid hydrate reduction by xanthine-xanthine oxidase. *Anal. Biochem.* **1997**, *251*, 206–209.
(21) Bartosz, G. Use of spectroscopic probes for detection of reactive oxygen species. *Clin. Chim. Acta* **2006**, *368*, 53–76.
(22) Haag, W. R.; Hoigne, J. Photo-sensitized oxidation in natural-water via ·OH radicals. *Chemosphere* **1985**, *14*, 1659–1671.
(23) Cho, M.; Chung, H.; Choi, W.; Yoon, J. Linear correlation between inactivation of E-coli and OH radical concentration in TiO_2 photocatalytic disinfection. *Water Res.* **2004**, *38*, 1069–1077.
(24) Elovitz, M. S.; von Gunten, U.; Kaiser, H. P. Hydroxyl radical/ozone ratios during ozonation processes. II. The effect of temperature, pH, alkalinity, and DOM properties. *Ozone-Sci. Eng.* **2000**, *22*, 123–150.
(25) Pickering, K. D.; Wiesner, M. R. Fullerol-sensitized production of reactive oxygen species in aqueous solution. *Environ. Sci. Technol.* **2005**, *39*, 1359–1365.
(26) Maurette, M. T.; Oliveros, E.; Infelta, P. P.; Ramsteiner, K.; Braun, A. M. Singlet oxygen and superoxide - experimental differentiation and analysis. *Helv. Chim. Acta* **1983**, *66*, 722–733.
(27) Wilkinson, F.; Helman, W. P.; Ross, A. B. Rate constants for the decay and reactions of the lowest electronically excited singlet state of molecular oxygen in solution-an expanded and revised compilation. *J. Phys. Chem. Ref. Data* **1995**, *24*, 663–1021.
(28) Joshi, A.; Punyani, S.; Bale, S. S.; Yang, H. C.; Borca-Tasciuc, T.; Kane, R. S. Nanotube-assisted protein deactivation. *Nat. Nanotechnol.* **2008**, *3*, 41–45.
(29) Barone, P. W.; Baik, S.; Heller, D. A.; Strano, M. S. Near-infrared optical sensors based on single-walled carbon nanotubes. *Nat. Mater.* **2005**, *4*, 86–U16.
(30) Curran, S. A.; Talla, J. A.; Zhang, D.; Carroll, D. L. Defect-induced vibrational response of multi-walled carbon nanotubes using resonance raman spectroscopy. *J. Mater. Res.* **2005**, *20*, 3368–3373.
(31) Wang, C. C.; Zhou, G.; Liu, H. T.; Wu, J.; Qiu, Y.; Gu, B. L.; Duan, W. H. Chemical functionalization of carbon nanotubes by carboxyl groups on stone-wales defects: A density functional theory study. *J. Phys. Chem. B* **2006**, *110*, 10266–10271.
(32) Huang, X.; Zhuang, Z. X.; Frenkel, K.; Klein, C. B.; Costa, M. The role of nickel and nickel-mediated reactive oxygen species in the mechanism of nickel carcinogenesis. *Environ. Health Perspect.* **1994**, *102*, 281–284.
(33) Lu, H. T.; Shi, X. L.; Costa, M.; Huang, C. S. Carcinogenic effect of nickel compounds. *Mol. Cell. Biochem.* **2005**, *279*, 45–67.
(34) Halliwell, B.; Gutteridge, J. M. C. Oxygen-toxicity, oxygen radicals, transition-metals and disease. *Biochem. J.* **1984**, *219*, 1–14.

ES101073P